SCIRES it
SCIentific RESearch and Information Technology
Ricerca Scientifica e Tecnologie dell'Informazione
Vol 12, Issue 2 (2022), 69-76
e-ISSN 2239-4303, DOI 10.2423/i22394303v12n2p69

CASPUR-CIBER Publishing, http://www.sciresit.it

APPLICATION OF HYPER-SPECTRAL IMAGING TECHNIQUE FOR COLORIMETRIC ANALYSIS OF PAINTINGS

Marcello Picollo, Andrea Casini*, Costanza Cucci*, Filippo Cherubini*, Lorenzo Stefani**

*Istituto di Fisica Applicata "Nello Carrara", Consiglio Nazionale delle Ricerche (IFAC-CNR) - Florence, Italy

Abstract

This paper describes the Hyper-Spectral Imaging (HSI) scanner developed at IFAC-CNR for non-invasive diagnostics and accurate color acquisitions on paintings. This latter HSI application is still rare in the art conservation field due to the difficulties related to obtaining accurate, reliable, and reproducible data suitable for matching the colorimetric calculations as required by the Commission Internationale de l'Eclairage (CIE) for calibrated sRGB images and colorimetric values are presented. In the present paper, HSI measurements focused on color evaluation of color standards in laboratory and of a 15th century panel painting are reported.

Keywords

Hyper-spectral imaging technique, color measurement, CIEL*a*b*, sRGB, painting restoration

1. *Introduction*

Hyper-Spectral Imaging (HSI), which can be used in different applicative contexts, enables the acquisition of data sets that include hundreds of spectral images acquired in very narrow spectral bands (bandwidth 2–10 nm). It is a technique that can be implemented with different imaging spectroscopy systems to meet the needs required in the various fields; for applications in cultural heritage (CH), for example, it mainly operates in reflectance mode (Cucci, Delaney, & Picollo, 2016; Striova, Dal Fovo, & Fontana, 2020). Moreover, depending on the type of sensor, it covers the Visible (Vis), Near Infrared (NIR), and Short-Wave Infrared (SWIR) regions (Cucci et al., 2016). The data obtained with HSI allow the reconstruction of a reflectance spectrum of each pixel in the scene, thus providing laboratory-like spectroscopic information that can be used for identification purposes. In addition, by means of these spectral data it is possible to group and map materials according to their spectral similarities (Cucci et al., 2016; Bai, Messinger, & Howell, 2019; Deborah, George, & Hardeberg, 2019). This is possible using algorithms that reduce the dimensionality of data and extract the required information. These algorithms included Principal Component Analysis (PCA) and Maximum Noise Fraction (MNF), or automated classification methods, such as neural networks, t-Distributed Stochastic Neighbor Embedding (t-SNE) and Uniform Manifold Approximation and Projection for Dimension Reduction (UMAP)(Kruse, Lefko, Boardman, Heidebrecht, Shapiro, Barloon, & Goetz, 1993; Mardia, Kent, & Bibby, 1979; Martens, & Naes, 1989; McInnes, Healy, & Melville, 2018). The results can be expressed as images in which material distributions are mapped, thus enhancing aspects that may not be detectable by visual inspection.

In addition, HSI technique can be used for high quality archival documentation of art works in terms of image quality, spatial sampling, and color accuracy. These terms can be satisfied if the acquired data meet the requirements established by curators and conservators with HSI instrumentation adapted to their protocols. In addition, illumination and observation geometry configurations have to follow the Commission Internationale de l'Eclairage (CIE) recommendations, such as the 45° / 0° and d / 0° configurations, to provide calibrated RGB images (sRGB) and colorimetric values (i.e., CIEXYZ, CIEL*a*b*, sRGB, etc.) (Marcus, 1998; Berns, 2001; Martinez, Cupitt, Saunders, Pillay, 2002; CIE, 2004; Burger and Burge, 2009; Cucci, Casini, Picollo, Poggesi, & Stefani, 2011).

It is still rare to find HSI technique applied to colorimetric analysis of paintings, for instance before and after their restoration. This is due to the difficulties in acquiring mutually comparable data, such as making sure that in each data set the pixel sizes are homogeneous with each other, the illumination is evenly distributed over the analyzed surface, the reference white measurement is constant over time, etc. (Picollo, Cucci, Casini, & Stefani, 2020).

In early 2000, IFAC-CNR designed and assembled an HSI scanner for the noninvasive study of flat objects, such as paintings (Fig. 1) (Casini, Bacci, Cucci, Lotti, Porcinai, Picollo, Radicati, Poggesi, & Stefani, 2005). This HSI system was also designed to enable the acquisition of data that could be used to obtain colorimetric values according to CIE guidelines. In this way, it was possible to obtain color (sRGB) images faithful to those acquired from RGB cameras. This first prototype has since been implemented to cover both the visible and near infrared (400-900 nm, VNIR) and short wave infrared (950-1650 nm, SWIR) (Cucci et al., 2016). At the same time, different HSI scanners were built to analyze different families of objects, from large-scale paintings to photographic negatives and positives. The measurements centering on the color analysis of a 15th-century panel painting, before and after the challenging restoration operations, will serve as a case study for illustrating the application of HSI in the field of fine art conservation.

2. *Experimental*

IFAC-CNR developed a pushbroom HSI system consisting of a linear scanner formed of an orthogonal pair of linear motion actuators that move a hyperspectral head in a vertical plane. The components of the head are an ORCA-ER CCD camera (Hamamatsu), a spectrograph (Specim V10E) with very negligible geometric deformations and additional filters for internal diffuse light compensation, and a telecentric lens (Opto-Engineering). The system operates in the 400-900 nm spectral range with an optical module optimized to minimize errors and distortions in the acquired image that may be caused by the non-planarity of the painting and its surface defects. The telecentric lens is able to perform parallel projection within ~ 3cm depth. This feature is critical for close range scanning in order to avoid parallax errors. It also has an impact on the precision in joining adjacent scan lines, even in situations in which the paint surface may not be flat. The telecentric depth tolerance eases the correct positioning of the scanner in relation to the painting by the aid of line laser pointers. Slightly overlapping, 60 mm wide vertical strips are scanned at a constant velocity of 1.5 mm / sec, with the camera operating at 16.7 frames per second in 2x2 binning mode.

The 3300 K QTH source emits radiation, which is sent via an optical fiber illuminator (Schott-Fostec) on an optical fiber bundle ending with a pair of cylindrical lenses. The function of these is to focus the radiation symmetrically at 45° with respect to the normal to the surface, as recommended by CIE (Fig. 2).

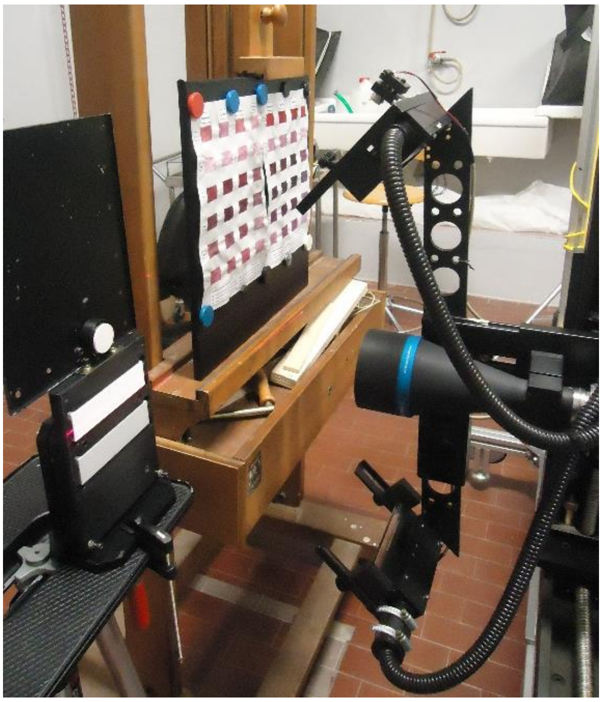

Fig. 1: IFAC-CNR spectrographic imaging head with the lighting module during the acquisition of HSI data.

Colorimetric errors may occur, due to the spectrograph internal straylight, which is isolated from external light. For the IFAC-CNR HSIs system, it was roughly compensated making an undercorrection by simply subtracting the signal collected below 400 nm. This signal must be null since no signal is expected in that spectral region because a high performance 389 nm long pass filter has been inserted in the telecentric lens for blocking the radiation below 400 nm before the spectrograph. Precise stray light correction algorithms are described in literature for spot spectroradiometers but they require the knowldege of the stray light wavelength response function (Zong, Brown, Johnson, Lykke, & Ohno, 2006). These procedures resulted to be heavy when applied to the massive data of a field instrument like this one, especially if they have to be extended to the second spatial dimension of the line spectrograph.

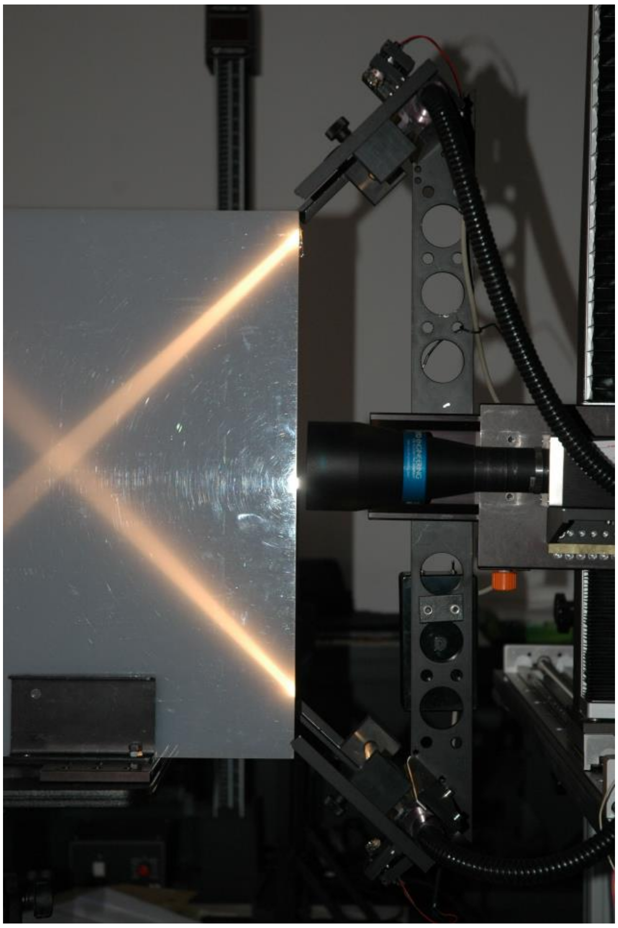

Fig. 2: Sectional visualization of the obtained light patterns.

The spatial resolution is evaluated at 50% contrast reduction and is greater than 2 lines/mm at all wavelengths in the 400-900 nm range with spatial sampling rate of the system is 11 lines/mm (279 ppi). The spectral acquisition step is 1.25 nm that gives a full width at half-maximum resolution of 2.55 nm.

In order to circumscribe any possible cause of damage on artworks due to light exposure, the maximum illumination of ~ 16000 lux and UVA fraction of approximately 56 μW/lumen were verified under typical measurement conditions (scan at 1.5mm/sec). When dealing with light sensitive and faded materials the high peak value suggests caution, and the resulting total exposure to light is less than 500 luxhr, which can be considered a fair value regarding the risks of photo-degradation (Thomson, 1986).

The use of the IFAC-CNR HSI device follows a standardized experimental acquisition protocol that guarantees comparability of different measurement sessions concerning reproducibility of illumination, data-acquisition, repositioning, etc., since all the data are acquired with the same measurement setup and methodology (Figs. 1 and 2).

For the calculation, the spectral data acquired by the HSI system were interpolated from 1.25 nm to 1 nm using an "in house" program developed at IFAC-CNR. As a result, grayscale TIFF format images were obtained for each of the three coordinates L*, a* and b* defined for the 2° standard observer and illuminant D65 (Cherubini, Casini, Cucci, Picollo, & Stefani, 2022).

Tab. 1: Color difference for the SCT comparing the CIEL*a*b*1976 color values provided by the produced and those calculated from the IFAC HSI scanner for 2° Standard Observer and D65 illuminant.

Spectralon Color Target (SCT)	SCT Color difference (ΔE_{00})
red	1.87
green	1.25
blue	1.05
yellow	1.57
cyan	0.72
orange	0.98
purple	0.59
violet	0.53

This methodological approach was used to process the data acquired on the Spectralon™ color standards (SCT) to verify the color accuracy of the data thus acquired. Here, the colorimetric values were calculated starting from spectra which were the average of 9x9 pixels. The obtained results were very promising: indicatively, a $\Delta E_{00} = 2.0$ was taken as the reference limit value below that the colorimetric data were considered acceptable, as reported in table 1, taking into consideration that the certified data were obtained with a different measurement geometry (0°/d). However, it is surprisingly high the ΔE_{00} value for the red target.

3. *Case study*

The HSI data were acquired before and after the restoration of the 15th century egg tempera panel painting *Saint John, Tobiolo and angel* (124.5 cm x 74.5 cm) by anonimous to study the colorimetric variations of the painted surface following the restoration treatment. The HSI data after cleaning (T1) was resized so that each pixel of the data corresponded to that of the HSI data acquired before restoration (T0). This operation consists of aligning the x=0 and y=0 values for the two data sets, which turns out simple and does not involve having to rescale the entire two data packages. This operation is necessary whenever the painting and/or the scanner are moved between the two measurements. This step is essential in order to compare the extracted reflectance spectra of each pixel, or pixel average, from the HSI data acquired at different times. The colorimetric data were stored as CIEL*a*b*76 images (in TIF format) files that enabled the visualization of the three-color parameters (L*, a*, b*) as three separated grey level maps, in which high values for the three parameters corresponded to brighter pixels in the resulting image file. The colorimetric values were calculated for the 2° Standard Observer and D65 illuminant (Cherubini et al., 2022). Figure 3 presents the sRGB image reconstructed of a detail of the panel painting before and at the end of the cleaning procedure and the removal of previously restored areas.

Before the restoration intervention, the appearance of the painting's colors was altered by the presence of the old varnish, which was yellowed and with a greyish patina. In addition, there were many repaintings made in previous restorations, which have been removed during the present intervention. This fact has determined that the color parameters have changed to varying extent depending on the areas of the paintings. To better visualize the results on the painting after the removal of the aged varnish and the old restored areas, CIE colorimetric values, L*, a* and b*, were used to monitor the chromatic changes of the paint layers due to the restoration intervention.

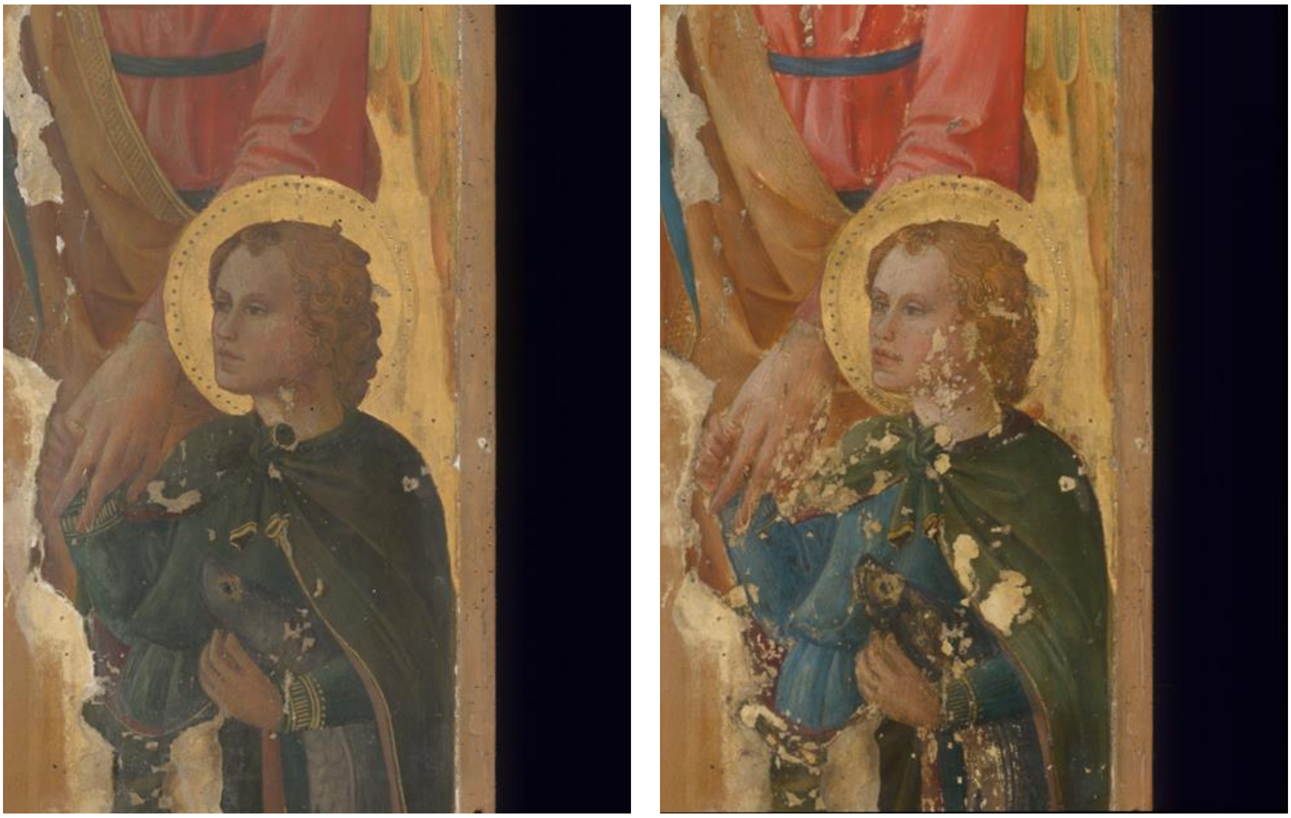

Fig. 3: sRGB detail of the painting reconstructed from the HSI data before (left) and after (right) the restoration procedure.

Before the restoration intervention, the appearance of the painting's colors was altered by the presence of the old varnish, which was yellowed and with a greyish patina. In addition,

there were many repaintings made in previous restorations, which have been removed during the present intervention. This fact has determined that the color parameters have changed to varying extent depending on the areas of the paintings. To better visualize the results on the painting after the removal of the aged varnish and the old restored areas, CIE colorimetric values, L*, a* and b*, were used to monitor the chromatic changes of the paint layers due to the restoration intervention.

As expected, the color variations following the intervention affected each colorimetric value and the final color differences were calculated with the ΔE_{00} equation (Sharma, Wu, & Dalal, 2005). Table 2 shows the values calculated on seven pixels corresponding to blue, green, yellow, red and skin tones, as reported in figure 4. The removal, or selective thinning, of the altered varnish first determined significant variations of the L* parameter. It exhibits higher values after cleaning, since the gray film component on top of the paint film has been reduced.

Tab. 2: Colorimetric values (L*, a*, b* and C*) on seven selected spots calculated from the spectra extracted by the HSI files acquired before (T0) and after (T1) the restoration process. CIE 2° Standard Observer and D65 illuminant, CIEDE2000 color difference formaulae (Sharma et al., 2005).

Spot #	Space coordinates (x, y)	L*		a*		b*		ΔC*	ΔE_{00}
		T0	T1	T0	T1	T0	T1		
1	190 / 160	40.94	50.64	14.94	25.35	17.23	21.23	10.26	29.19
2	217 / 076	33.38	37.11	-2.13	-3.53	1.93	-9.19	1.57	18.55
3	330 / 351	44.60	48.35	9.30	12.96	18.24	24.69	7.41	31.00
4	260 / 410	39.85	42.72	17.04	28.10	17.16	28.28	15.68	37.25
5	120 / 219	40.12	47.84	11.92	17.83	21.18	34.60	14.62	34.22
6	177 / 631	29.32	39.11	-3.43	-6.31	2.90	-2.58	2.33	9.91
7	479 / 580	21.92	21.83	-0.09	-3.21	4.09	11.87	8.21	6.72

Fig. 4: sRGB detail of the painting after the removal of the old varnish and previous repaintings showing the points where the reflectance spectra were extracted from the HSI data for the calculation of the colorimetric parameters.

Fig. 5: sRGB details before (left) and after (right) of the removal of the old varnish of the painting to better visualize the dramatic color changes of the face of Tobiolo and the mantle of the angel (spots 3-5).

Depending on the colors of the areas, the removal of the aged varnish, which had a non-negligible yellow component, resulted in a reduction in the values of the parameter b* (blue–yellow component) for blue spot 2. The other colors (complexion, yellow, red and green), instead, showed the opposite behavior as the b* values increased. This result confirms that the removal of the aged varnish also changed the saturation of the colors, as also confirmed by the parameter a* (red–green component), which always presented higher absolute values than before cleaning. For completeness of information, the chroma differences (ΔC^*) for the seven selected spots are reported in Table 2.

As expected, the ΔE_{00} values were particularly high, with the exception of points 6 and 7 where these values were found to be lower than 10.

The images of the a* colorimetric values calculated for the CIEL*a*b*1976 color space before and after the restoration are reported in Figure 6. Here the high gray scale areas highlight pixel with positive a* values while the low gray scale areas evidenced the pixel with negative a* values.

4. *Final considerations*

The HSI reflectance technique has been applied only on a few occasions on paintings for colorimetric measurements. In fact, it is not easy to have HSI systems that ensure repeatable and reproducible measurement methods and that meet the recommendations of the CIE for monitoring any color variations.

These systems must have a lighting / recording system with fixed measurement geometry (such as 0° / 45°) and maintain the same spatial resolution for measurements acquired at different times of the same detail, so as to be able to perfectly superimpose the pixels of the two datasets.

Furthermore, HSI systems must be built in such a way as to minimize stray light and glare problems, as well as those of chromatic aberration and geometric deformations due to the optics used.

However, once these problems have been solved or minimized, the possibility given by HSI systems to combine images with good resolution and spectral data consents to calculate the colorimetric values for each pixel of the image and therefore to be able to accurately map the distribution of the colorimetric values over the entire area under study. This possibility, in the case of paintings surface cleaning, allows to precisely quantify the selective thinning work of the altered paints, the removal of previous repaintings, the evaluation of possible metamerism problems, the evaluation of the effect of new paints and to follow their behavior over time, etc., by the colorimetric values.

Fig. 6: images in grey scale of a* colorimetric values before (left) and after (right) restoration.

References

Bai, D., Messinger, D.W., & Howell, D. (2019). A hyperspectral imaging spectral unmixing and classification approach to pigment mapping in the Gough & Selden Maps. *J. Am. Inst. Conserv.*, 58, 68–89.

Berns, R. S. (2001). The science of digitizing paintings for color-accurate image archives: a review. *Journal of imaging science and technology*, 45(4), 305-325.

Burger, W., & Burge, M. J. (2010). *Principles of digital image processing: core algorithms*. Springer Science & Business Media.

CIE. 15:2004. Technical Report. Colorimetry, 3rd ed.; Commission International de I'Eclairage (CIE), Central Bureau of the CIE: Vienna, Austria.

Casini, A., Bacci, M., Cucci, C., Lotti, F., Porcinai, S., Picollo, M., Radicati, B., Poggesi, M., & Stefani, L. (2005, August). Fiber optic reflectance spectroscopy and hyper-spectral image spectroscopy: two integrated techniques for the study of the Madonna dei Fusi. In: *Optical Methods for Arts and Archaeology* (Vol. 5857, pp. 177-184) SPIE.

Cucci, C., Casini, A., Picollo, M., Poggesi, M., & Stefani, L. (2011, June). Open issues in hyperspectral imaging for diagnostics on paintings: When high-spectral and spatial resolution turns into data redundancy. In *O3A: Optics for Arts, Architecture, and Archaeology III* (Vol. 8084, pp. 57-66). SPIE.

Cucci, C., Delaney, J. K., & Picollo, M. (2016). Reflectance hyperspectral imaging for investigation of works of art: old master paintings and illuminated manuscripts. *Accounts of chemical research*, 49(10), 2070-2079.

Cherubini, F., Casini, A., Cucci, C., Picollo, M. & Stefani, L. (2022). Application of a hyperspectral camera for colorimetric measurements on polychrome surfaces in a controlled environment and evaluation of three image processing software for displaying colorimetric data: Pros and cons of the methodology presented. *Color Research and Application*. https://doi.org/10.1002/col.22835.

Deborah, H., George, S., & Hardeberg, J.Y. (2019). Spectral-divergence based pigment discrimination and mapping: A case study on The Scream (1893) by Edvard Munch. *J. Am. Inst. Conserv.*, 58, 90–107.

Kruse, F.A., Lefko, A.B., Boardman, J.B., Heidebrecht, K.B., Shapiro, A.T., Barloon, P.J., & Goetz, A.F.H. (1993). The spectral image processing system (SIPS)—Interactive visualization and analysis of imaging spectrometer data. *Remote Sens. Environ.*, 44, 145–163.

Marcus, R.T. 1998. The measurement of color. In K. Nassau (Ed.), *Color for Science, Art and Technology* (31-96). Amsterdam: Elsevier.

Mardia, K.V., Kent, J.T., & Bibby, J.M. (1979). *Multivariate Analysis*. London: Academic Press.

Martens, H., & Naes, T. (1989). *Multivariate Calibration*. New York: Wiley and Sons.

Martinez, K., Cupitt, J., Saunders, D., & Pillay, R. (2002). Ten years of art imaging research. *Proceedings of the IEEE*, 90(1), 28-41.

McInnes, L., Healy, J., & Melville, J. (2018). UMAP: Uniform manifold approximation and projection for dimension reduction. arXiv 2018, arXiv:1802.03426v2.

Picollo, M., Cucci, C., Casini, A., & Stefani, L. (2020). Hyper-Spectral Imaging Technique in the Cultural Heritage Field: New Possible Scenarios. *Sensors*, 20(10), 2843. https://doi.org/10.3390/s20102843

Sharma, G., Wu, W., & Dalal, E. N. (2005). The CIEDE2000 color-difference formula: Implementation notes, supplementary test data, and mathematical observations. *Color Research & Application*: Endorsed by Inter-Society Color Council, The Colour Group (Great Britain), Canadian Society for Color, Color Science Association of Japan, Dutch Society for the Study of Color, The Swedish Colour Centre Foundation, Colour Society of Australia, Centre Français de la Couleur, 30(1), 21-30.

Striova, J., Dal Fovo, A., & Fontana, R. (2020). Reflectance imaging spectroscopy in heritage science. *La Rivista del Nuovo Cimento*, 43(10), 515-566.

Thomson, G. (1994). *The museum environment* / Garry Thomson. (2nd ed. / paperback ed., Butterworth-Heinemann series in conservation and museology). Oxford: Butterworth Heinemann in association with The International Institute for Conservation of Historic and Artistic Works.

Zong, Y., Brown, S. W., Johnson, B. C., Lykke, K. R., & Ohno, Y. (2006). Simple spectral stray light correction method for array spectroradiometers. *Appl Opt.,* 45(6), 1111-1119.